

Testing Times for Supersymmetry: Looking Under the Lamp Post

Amol Dighe,¹ Diptimoy Ghosh,² Ketan M. Patel,¹ and Sreerup Raychaudhuri¹

¹*Department of Theoretical Physics, Tata Institute of Fundamental Research, Mumbai 400 005, India.*

²*INFN, Sezione di Roma, Piazzale A. Moro 2, I-00185 Roma, Italy.*

We make a critical study of two highly-constrained models of supersymmetry — the constrained minimal supersymmetric standard model (cMSSM), and the non-universal Higgs mass model (NUHM) — in the light of the 125-126 GeV Higgs boson, the first observation of $B_s \rightarrow \mu\mu$ at the LHCb, and the updated $B \rightarrow \tau\nu$ branching ratio at BELLE. It turns out that these models are still allowed by the experimental data, even if we demand that there be a light stop with mass less than 1.5 TeV. The only significant effects of all these constraints are to push the mass of the light stop above ~ 500 GeV, and to prefer the universal trilinear coupling A_0 to be large and negative. We calculate the Higgs boson branching ratios to $WW, ZZ, \tau\tau$ and $\gamma\gamma$ in these models and show that improved experimental limits on these could put them to the most stringent experimental tests yet.

PACS numbers: 12.60.Jv, 13.85.Rm, 14.80.Ly, 14.80.Nb

The recent discovery [1], at the CERN LHC, of a boson with mass around 125-126 GeV and properties closely resembling those of the Standard Model (SM) Higgs boson [2, 3], matches well with a common prediction of all supersymmetric models [4], viz., the existence of a light Higgs boson with mass in the 100 – 135 GeV range. However, as this could be sheer coincidence, only the discovery of a superpartner of one of the known SM particles would really establish the existence of supersymmetry (SUSY). Now, the elevation of the light Higgs boson mass to a value above $M_Z \approx 91$ GeV in supersymmetric models is known [4] to be primarily due to radiative corrections involving the top quark (t) and the light and heavy stop states (\tilde{t}_1, \tilde{t}_2). It follows, therefore, that the discovery of a light Higgs boson candidate in the upper part of the SUSY-allowed range may be considered as a hint of the existence of a rather low-lying stop state (\tilde{t}_1) — perhaps light enough to be discovered at the LHC. We cannot, however, be too sure about this, for SUSY models can be practically indistinguishable from the SM if we take the so-called *decoupling limit*, where all the superpartners are too heavy to be detected at the LHC (or any terrestrial experiment conceivable in the near future).

Faced with this situation, we approach the problem in a pragmatic way, viz. we focus on that part of the large SUSY parameter space that could support a light stop state *discoverable at the LHC*. Though this does resemble the proverbial search under the lamp post, at the present juncture, it seems the most reasonable thing to do. The question then arises as to how light the \tilde{t}_1 state must be. An exact answer is, of course, a matter of detail, but one can form a crude estimate based on the fact that the production of $\tilde{t}_1\bar{\tilde{t}}_1$ pairs at the LHC is dominated by strong interactions and hence depends essentially on the mass of the \tilde{t}_1 alone. The variation of the $\tilde{t}_1\bar{\tilde{t}}_1$ pair-production cross-section with $m_{\tilde{t}_1}$ at the 14-TeV LHC is easily calculated [5], and this falls from a few pb at $m_{\tilde{t}_1} \simeq 300$ GeV to about 10 ab for $m_{\tilde{t}_1} \simeq 1.5$ TeV. As a typical estimate of the integrated luminosity of the LHC is about 3 ab^{-1} ,

the latter value corresponds to around 30 $\tilde{t}_1\bar{\tilde{t}}_1$ pairs — which may be just enough for a discovery. Accordingly, we take $m_{\tilde{t}_1} \leq 1.5$ TeV as a reasonable criterion for a possible LHC discovery of the light stop.

This light stop criterion is not, however, the only restriction on the parameter space of the SUSY model in question. The requirement of a light Higgs state in the range 122 – 129 GeV, coupled with the recent observation of the rare decay $B_s \rightarrow \mu^+\mu^-$ [6], the updated $B \rightarrow \tau\nu$ branching ratio at BELLE [7], and the negative results of all direct searches for new particles at the LHC [8], taken together, make a formidable combination, imposing tight restrictions on models of new physics. Among the most severely affected are models where the electroweak sector differs from that of the SM. All SUSY models fall in this class. In an article [9] written last summer, just before the announcement of the new boson discovery, two of the present authors had shown that even the most restrictive model of supersymmetry, viz. the constrained Minimal Supersymmetric SM (cMSSM) [4], was affected by the then-available data only marginally — at the periphery of its parameter space — leaving most of its parameter choices viable. The new data obtained since then have, in the span of a few months, changed the situation quite dramatically — the allowed parameter space now appears to be severely restricted [10].

Since the new data are all compatible with the SM, they may be expected to drive SUSY towards the decoupling limit. This, of course, runs contrary to the light stop scenario desired by us. In the current article, we examine whether the cMSSM can accommodate these conflicting requirements. Moreover, we also consider a popular extension of the cMSSM, known as the Non-Universal Higgs Mass (NUHM) model [11], which could, in principle, evade some of the constraints which affect the cMSSM adversely. Both the models in question have been widely discussed in the literature [12, 13], and do not require to be extensively reviewed in a focussed study such as the present one. Below, we just summarize

the principal motivation(s) and the parameter choices.

The cMSSM is a theoretically well-motivated supersymmetric model with the least number of parameters, and consequently has the highest predictivity of all low-energy SUSY models. The free parameters of this model are (i) the universal fermion mass $m_{1/2}$ at the grand unification (GUT) scale, (ii) the universal trilinear coupling A_0 at the GUT scale, (iii) the ratio $\tan\beta$ of vacuum expectation values of the two Higgs doublets at the electroweak scale, and (iv) the universal scalar mass m_0 at the GUT scale. In addition, we can choose the sign of the Higgs mixing parameter μ to be positive or negative.

Predictivity is the most appealing feature of the cMSSM, though it also makes it more vulnerable to all sorts of experimental constraints. Therefore, even if the cMSSM is ruled out by the data — or, more likely, pushed to its decoupling limit — it would be logical to look for its close cousins, *i.e.* models which contain at least some of the more attractive features of the cMSSM. The NUHM model is perhaps the most natural of these choices, for all that it does is to relax one of the cMSSM conditions and make the two Higgs mass parameters M_{h_1} and M_{h_2} different from the universal scalar mass m_0 at the GUT scale.

In our numerical studies, we study the independent variation of these parameters in the ranges

$$\begin{aligned} m_{1/2} &\in [0, 2] \text{ TeV}, & m_0 &\in [0, 5] \text{ TeV}, \\ A_0 &\in [-10, 10] \text{ TeV}, & \tan\beta &\in [5, 60], \\ M_{h_1} &\in [0, 5] \text{ TeV}, & M_{h_2} &\in [0, 5] \text{ TeV}, \end{aligned}$$

which are compatible with theoretical considerations and cover the entire region which allows for a light stop t_1 of mass below 1.5 TeV. We also restrict ourselves to $\mu > 0$, since only the positive sign of μ can ameliorate the 3.6σ disagreement of the SM with the measurement of the anomalous magnetic moment $(g-2)_\mu$ of the muon [8]. However, as it is still not possible to be compatible with the $(g-2)_\mu$ measurement to better than 95% C.L. [14], we choose to be conservative and do not impose this particular constraint in any other way. Having chosen the parameter ranges, then, we make a random scan over the entire range of these variables. For each set of input parameters, we use the public domain software SUSY-HIT [15] to compute the values of the entire supersymmetric spectrum and couplings at the respective scales at which the experimental data are available. These are then taken as inputs to calculate a slew of high- and low-energy observables for which experimental data are available. For this part, we use the software SUPERISO [16] and FEYNHIGGS [17].

In order to constrain the parameter space, we first impose the “theory” constraints, *i.e.* the obvious requirement that the electroweak symmetry be broken at precisely the electroweak scale, and the requirement that the

lightest sparticle be neutral (which arises from its identification as a dark matter candidate). However, taking a conservative stance again, we do not impose constraints arising from the relic density of this neutralino, since such constraints can be evaded in scenarios with non-thermal dark matter [18]. In addition, we use the following constraints, many of which have been recently updated (mostly during 2012):

(i) The mass of the lightest Higgs boson M_h lies in the narrow range $122.5 \text{ GeV} < M_h < 129.5 \text{ GeV}$. This range includes the 95% C.L. errors from the ATLAS and CMS data [1] as well as a 1.5 GeV theoretical uncertainty [19].

(ii) The branching ratios \mathcal{B} for some rare B decays are constrained as follows, at 95 % C.L. [6, 20, 21]

$$\begin{aligned} 1.1 \times 10^{-9} &< \mathcal{B}(B_s \rightarrow \mu^+ \mu^-) < 6.4 \times 10^{-9}, \\ &\mathcal{B}(B_d \rightarrow \mu^+ \mu^-) < 9.4 \times 10^{-10}, \\ 2.6 \times 10^{-4} &< \mathcal{B}(B \rightarrow X_s \gamma) < 4.5 \times 10^{-4}, \\ 0.44 \times 10^{-4} &< \mathcal{B}(B \rightarrow \tau \nu_\tau) < 1.48 \times 10^{-4}. \end{aligned}$$

As a matter of fact, the first measurement of $\mathcal{B}(B_s \rightarrow \mu\mu)$ has recently been reported at the LHCb [6]. Also, the measurement of $\mathcal{B}(B \rightarrow \tau\nu)$ with hadronic tag has recently been updated by BELLE [7] and brings the value of this ratio to a much smaller value than earlier measured. This not only relaxes the tension of this measurement with the SM prediction, but also dissipates the strong constraints it had put on the cMSSM [22]. Here we take the BELLE average of $\mathcal{B}(B \rightarrow \tau\nu)$ [21].

(iii) Another low energy measurement arises from the 2006 measurement, at the DAΦNE facility at Frascati, of the process $K^+ \rightarrow \mu^+ \nu_\mu$. Taking the 95% C.L. limits, this gives us [23]

$$0.6331 < \mathcal{B}(K^+ \rightarrow \mu^+ \nu_\mu) < 0.6401,$$

which can be very restrictive for a certain class of electroweak models.

(iv) We also impose the 95% C.L. lower bounds on the masses of sparticles, as listed by the Particle Data Group (PDG) [8]. These are given below, with all masses being measured in GeV:

$$\begin{aligned} M_{\tilde{\chi}_1^0} &> 46, & m_{\tilde{q}} &> 1100, & m_{\tilde{\ell}} &> 107, \\ M_{\tilde{\chi}_2^0} &> 116, & m_{\tilde{t}_1} &> 95.7, & m_{\tilde{\nu}_\ell} &> 94, \\ M_{\tilde{\chi}_1^\pm} &> 94, & m_{\tilde{b}_1} &> 89, & m_{\tilde{\tau}_1} &> 81.9, \\ M_{\tilde{g}} &> 500. \end{aligned}$$

Here \tilde{q} and $\tilde{\ell}, \tilde{\nu}_\ell$ refer to superpartners of the first two generations. There are more specific constraints on the gluino mass $M_{\tilde{g}}$, which depend on the mass $m_{\tilde{t}_1}$ of the light stop [8]; we have verified that these are satisfied for our allowed points.

Note that in selecting the allowed points in our random scan, we do not treat the early measurements of the Higgs boson branching ratios as constraints, since these are based on a rather small sample of Higgs boson decay

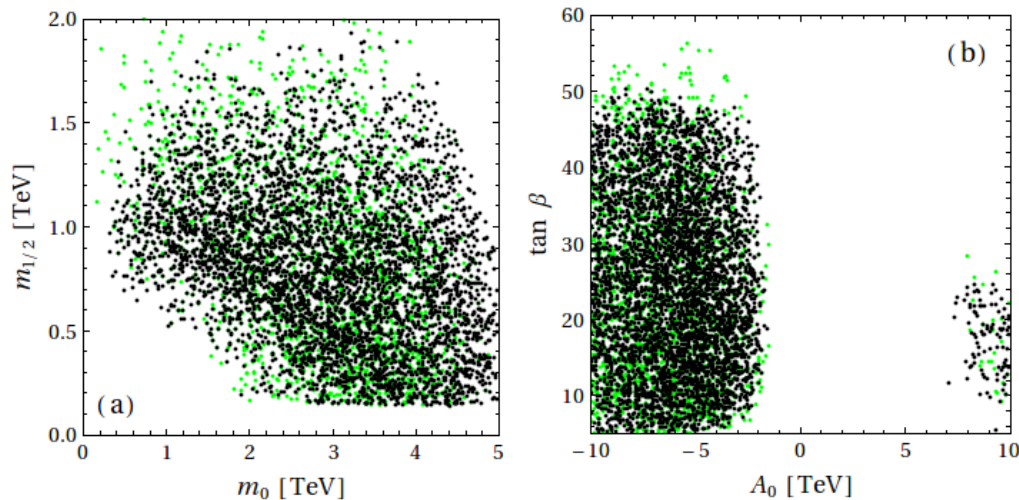


FIG. 1: Allowed regions in the parameter space for $\mu > 0$. We consider two sections of the parameter space, viz. (a) the $m_{1/2}$ - m_0 plane, and the (b) A_0 - $\tan\beta$ plane. The black dots indicate the cMSSM, while the green (grey) ones indicate the NUHM.

events and, consequently, have large error bars. Instead, we shall presently argue that these measurements could constitute stringent tests for the models in question as more data become available.

Taking all these constraints into account, the allowed points in our random scan are shown in Figure 1. The left panel — marked (a) — shows the m_0 - $m_{1/2}$ plane, while the panel on the right — marked (b) — shows the A_0 - $\tan\beta$ plane. We should note that all the parameters vary in these plots, *e.g.* in the panel (a), A_0 and $\tan\beta$ are not held fixed but are allowed to vary over the full ranges mentioned above. A glance at the panel (a) shows that the two models, viz. cMSSM and NUHM, hardly differ so far as the allowed region is concerned. Only in the so-called stau co-annihilation region, where m_0 is small and $m_{1/2}$ is large, does the NUHM enjoy a slightly more viable status than the cMSSM. However — and this is mostly due to the Higgs boson mass measurement — both the models are severely constrained in the low- m_0 and low- $m_{1/2}$ region. Unfortunately, this is also the region in which large signals for superpartners are predicted at collider machines, such as the LHC, so this result is unfavourable to the school of thought that supersymmetry is “around the corner”. The paucity of points in the “decoupling” region of large- m_0 and large- $m_{1/2}$ is a direct consequence of imposing the restriction $m_{\tilde{t}_1} \leq 1.5$ TeV. However, the large number of allowed points in the central region of the panel clearly indicates that these two models — with all their economy of parameter choices — are still capable of explaining all the experimental data, *as well as* predicting a light stop. This conclusion is also reflected in the panel (b), where it is clear that large negative values of A_0 are favored, but otherwise the only real restrictions are on large values of $\tan\beta$. These arise from the $\tan^6\beta$ sensitivity of

$\mathcal{B}(B_s \rightarrow \mu^+\mu^-)$ [24], coupled with the regime imposed by our artificial cutoff $m_{\tilde{t}_1} \leq 1.5$ TeV. In the cMSSM, this forces us to have $\tan\beta \lesssim 45$, but the NUHM can still have allowed points with larger $\tan\beta$ values.

It is interesting to ask why large negative values of A_0 are preferred. This is because the measured mass of the Higgs boson $M_h \simeq 125$ -126 GeV is sufficiently removed from the decoupling limit — typically quoted [4] as $M_h \approx 119$ GeV for $A_0 = 0$ — to require a light stop \tilde{t}_1 to explain that deviation. In order to sustain a light stop, while simultaneously keeping the squarks of the first two generations heavy, we require a large “seesaw” effect in the stop mixing matrix, and this happens when large negative values of A_0 appear in the off-diagonal terms of that matrix.

This is nicely illustrated in Fig. 2, where we have shown the scatter of parameter choices with the mass $m_{\tilde{t}_1}$ plotted against the A_0 parameter, and the effect of different classes of constraints on the allowed region in this plot. In panel (a), we impose only “theory” constraints, which are not only indifferent to the sign of A_0 , but also allow a stop lighter than 100 GeV in the $A_0 \approx 0$ region. In panel (b), we impose, in addition, the indirect constraints arising from low-energy measurements, including B-decays, and this immediately affects the $A_0 \approx 0$ region, driving the stop mass above 120 GeV. Imposition of the direct search constraints, especially the requirement that $m_{\tilde{q}} > 1.1$ TeV for the first two generations [8], cleans up the $A_0 \approx 0$ region in panel (c) much more efficiently, though a few points with a stop mass between 120-200 GeV still survive. Here, too, both signs of A_0 are equally preferred. However, when we impose the Higgs boson mass constraint, the allowed parameter space in panel (d) is affected quite severely. Not only are small values of A_0 completely washed-out, with A_0 being driven

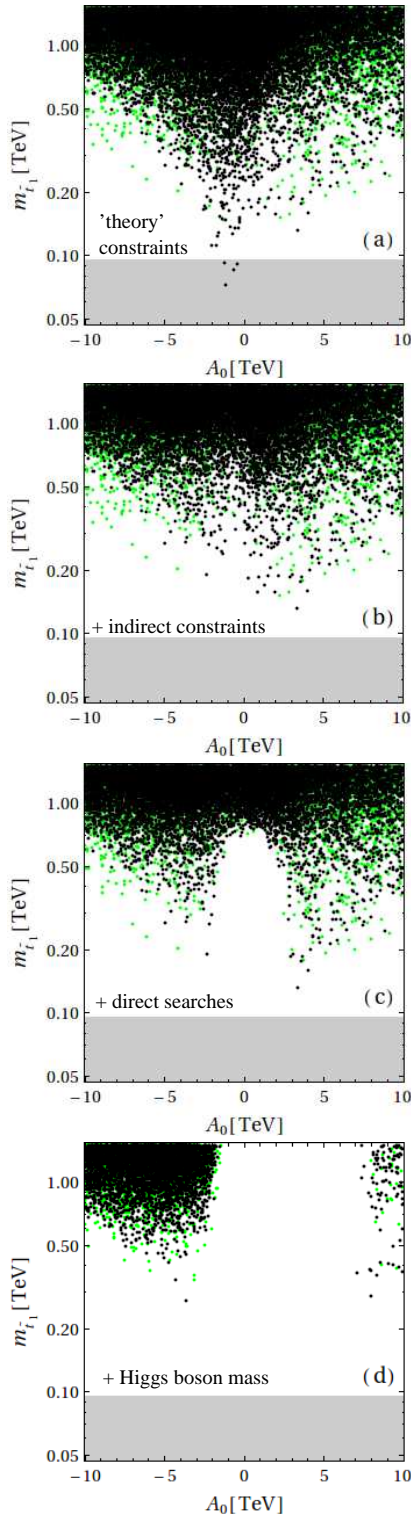


FIG. 2: Illustrating the correlation between the mass of the light stop and the A_0 parameter, as different sets of constraints are imposed successively. Each panel includes the constraints from the previous panel. The shaded region represents the LEP constraint on $m_{\tilde{t}_1}$. Other conventions followed are exactly the same as in Fig. 1.

below -2 TeV or above 8 TeV, but the stop mass is essentially pushed above 500 GeV, with only a few outlying points in the range 250-500 GeV (which may very well be due to specially fine-tuned cancellations). Thus there is no real surprise in the fact that experimental searches for stops lighter than 550 GeV at the 7-8 TeV LHC have come up empty-handed [25]. On the other hand, it is encouraging that there is a profusion of allowed points with a \tilde{t}_1 mass in the range 600 GeV–1 TeV — which, as we have argued, could easily turn out to be a happy hunting ground at the 14 TeV LHC.

We now come to the final test, viz, whether the models in question can predict the observed branching ratios of the Higgs boson as observed in the ATLAS [26] and CMS [27–30] data. Of course, what is observed at the LHC is not the branching ratio per se, but a number of events of a certain kind which can be identified as arising from the decay of a Higgs boson resonance. This corresponds to the convolution of the integrated luminosity \mathcal{L} with a production cross-section and a branching ratio, *i.e.* for a particle pair $X\bar{X}$, we have

$$N_{X\bar{X}} = \mathcal{L} \times \sigma(pp \rightarrow h^0) \times \mathcal{B}(h^0 \rightarrow X\bar{X}). \quad (1)$$

We then define the so-called *signal strength*

$$\mu_{X\bar{X}} \equiv \frac{N_{X\bar{X}}}{N_{X\bar{X}}^{\text{SM}}} = \frac{\sigma(pp \rightarrow h^0)}{\sigma_{\text{SM}}(pp \rightarrow h^0)} \times \frac{\mathcal{B}(h^0 \rightarrow X\bar{X})}{\mathcal{B}_{\text{SM}}(h^0 \rightarrow X\bar{X})}, \quad (2)$$

where the label SM indicates the SM predictions with $m_h = 126$ GeV. The Higgs production cross-sections are calculated using FEYNHIGGS and the branching ratios are calculated using the software HDECAY, which is incorporated in the SUSYHIT package and is used in conjunction with the supersymmetry parameters allowed by the constraints described above. Our results can then be compared with the latest experimental values of $\mu_{X\bar{X}}$ given by the two experimental collaborations [26–30], which are listed in Table I below.

	ATLAS	CMS
μ_{WW}	1.0 ± 0.3 [26]	0.76 ± 0.21 [27]
μ_{ZZ}	1.5 ± 0.4 [26]	$0.91^{+0.30}_{-0.24}$ [28]
$\mu_{\tau\tau}$	0.8 ± 0.7 [26]	1.1 ± 0.4 [29]
$\mu_{\gamma\gamma}$	1.6 ± 0.3 [26]	$0.78^{+0.28}_{-0.26}$ [30]

TABLE I: Experimental data on Higgs boson signal strengths, as reported in March 2013 by the ATLAS [26] and CMS [27–30] Collaborations. For $\mu_{\gamma\gamma}$ we use the multivariate analysis result from CMS [30].

From Table I, it is clear that at 95% C.L. all the measurements are compatible with a SM Higgs boson. We also note that these results are based on almost all the data collected in the 7–8 TeV run of the LHC, and hence, no substantial improvement may be expected till the energy/luminosity upgrade is in place.

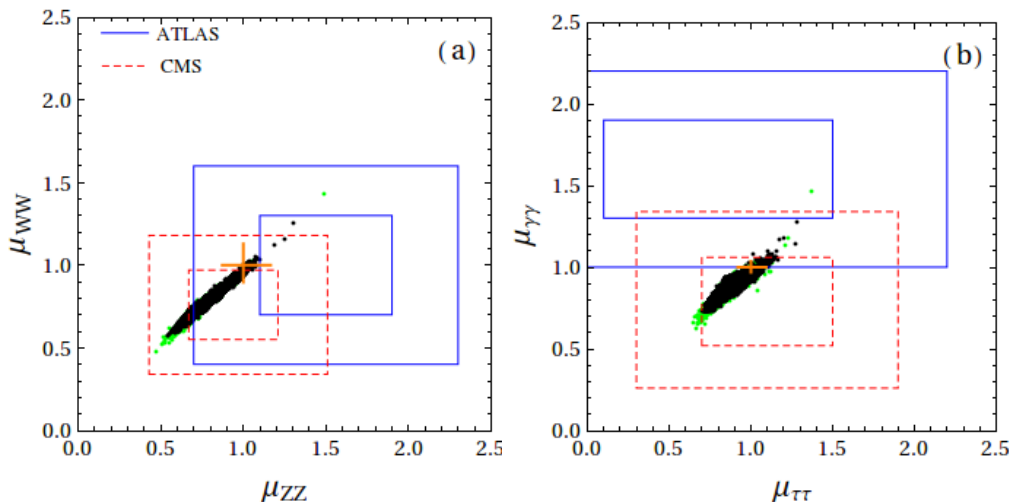


FIG. 3: Correlation plots for the signal strengths of the Higgs boson in different channels, vis-a-vis ATLAS and CMS bounds. SUSY conventions follow those of Fig 1. In each panel, the SM prediction lies at the crossing of the two short (orange) lines, which denote the theoretical uncertainty due to the spread in Higgs boson mass.

With these circumstances in mind, we now make a comparison between the signal strengths predicted in the cMSSM and the NUHM versus the experimental data. These results are shown in Fig. 3. In the panel on the left — marked (a) — we plot μ_{WW} versus μ_{ZZ} , with black dots indicating the cMSSM and green (grey) dots indicating the NUHM. The blue (solid line) boxes indicate the ATLAS limits at 1σ and 2σ respectively, while the red (dashed line) boxes indicate the CMS limits, again at 1σ and 2σ respectively. The SM prediction lies at (1.0, 1.0), i.e. at the crossing of the two short (orange/grey) lines, whose lengths correspond to the uncertainties arising from the allowed range in Higgs boson mass. It is immediately obvious that the CMS data are slightly more restrictive than the ATLAS data. If we take the bounds at 2σ , then it is obvious that the full scatter of points in both the cMSSM and NUHM are allowed by the data, as is, of course, the SM. On the other hand, if we consider the 1σ constraints, then the SM is disfavoured, whereas the two supersymmetric models survive.

The comparison changes a little if we turn to the panel on the right — marked (b). The conventions for this plot are exactly the same as before, the only difference being that we have plotted the more controversial $\mu_{\gamma\gamma}$ versus $\mu_{\tau\tau}$, the former being highly sensitive to new physics contributions. Here the ATLAS and CMS results are somewhat different. The SM point as well as the scatter of points in the two supersymmetric models lie in the heart of the CMS-allowed region, whereas for the ATLAS result, the SM lies at the 2σ border, while most of the supersymmetric points lie further out. Thus, in the ATLAS data, at least, there is some hint of new physics, but the CMS data appears to confound any such speculations.

It is quite clear from this study of the signal strengths that — as of now — both the cMSSM and NUHM survive

all the experimental tests, even if we demand a light stop state discoverable at the LHC. In fact, they do as well, if not better, than the SM — as is only to be expected from models with more free parameters. The predictions of these models in their allowed ranges may deviate significantly from the SM predictions; however the smallness of the scatter compared to the experimental errors in both the plots in Fig. 3 shows that, the present status of these models is not so different from that of the SM. Indeed, in both the panels of Fig. 3 the SM point lies right in the middle of a dense clustering of allowed SUSY points. This indicates that these two models can mimic the SM predictions for these signal strengths *even with a light stop* of mass $m_{\tilde{t}_1} \leq 1.5$ TeV. It is thus much too early to write off any model of supersymmetry, even the highly restrictive cMSSM.

As regards the future, one can only speculate. Obviously, when the results from the analysis of more data become available, the boxes in Fig. 3 will shrink, corresponding to a reduction in the experimental errors. Such changes are often accompanied by changes in the central value(s) as well, which would appear on the plots as a translation of the box(es) in some direction. Three distinct possibilities may now be considered.

(i) The new boxes may zoom in to the SM prediction. In this case our plots in Fig. 3 show that there are always points in the parameter space of the cMSSM and NUHM which will give the same $\mu_{X\bar{X}}$ predictions as the SM. Thus, these models will survive — and even predict a discoverable light stop — though with even more severe constraints on the parameter space.

(ii) The shrinking boxes may move away from the SM predictions, but stay within the scatter of allowed SUSY points shown in Fig. 3. This, would, of course, form a

powerful argument for these minimal versions of SUSY and would certainly enhance our expectations for a light stop discovery.

(iii) In addition, we must also consider the possibility that the new data will disfavour *both* the SM and these two highly-predictive SUSY models — in which case one would have to invoke less restrictive versions of SUSY (e.g. the 19-parameter pMSSM [10]) or other forms of new physics to explain the results.

Before concluding, we briefly consider the case when the “under the lamp post” restriction of $m_{\tilde{t}_1} \leq 1.5$ TeV is removed, or rendered irrelevant by negative results of direct stop searches at some time in the future. We find that relaxation of this requirement does not affect the low- m_0 and low- $m_{1/2}$ region, but does populate the high- m_0 and high- $m_{1/2}$ “decoupling” region. At the same time, high values of $\tan\beta$ are marginally less constrained. Moreover, small negative values of A_0 are now allowed, but we should note that these correspond only to heavier values of $m_{\tilde{t}_1} > 1.5$ TeV. More interestingly, the scatter of points in both panels of Fig. 3 does not change appreciably. It follows that our remarks about the future of tests involving Higgs boson decays would generally re-

main valid even with a heavy $m_{\tilde{t}_1}$, which may be beyond the kinematic reach of the LHC.

To sum up, then, we have made a critical study of two of the most restrictive models of supersymmetry, cMSSM and NUHM, taking into account the recent measurements of the Higgs mass and the updates in many flavour-physics observables. We find that these models can actually survive all the constraints and predict a light stop which could be discovered, in principle, at the LHC. The allowed parameter ranges for both the models seem almost identical, except for $\tan\beta$, which is restricted to be $\lesssim 45$ in the cMSSM with a light stop, while it could be larger in the NUHM. The branching ratios of the Higgs boson to $WW, ZZ, \tau\tau$ or $\gamma\gamma$ can be an important testing ground for the future of these models. However, as long as the experimental data do not exhibit definite disagreement with the SM, these SUSY models will continue to survive, and may even offer the exciting possibility of a light stop discovery in the coming runs of the LHC.

Acknowledgements: DG acknowledges support from ERC Ideas Starting Grant n. 279972 “NPFlavour”. He would also like to thank M. Guchait for discussions.

-
- [1] G. Aad *et al.* [ATLAS Collaboration], Phys. Lett. B **716**, 1 (2012) [arXiv:1207.7214 [hep-ex]]; S. Chatrchyan *et al.* [CMS Collaboration], Phys. Lett. B **716**, 30 (2012) [arXiv:1207.7235 [hep-ex]]; TEVNPH Working Group (for the CDF, D0 Collaborations), Fermilab preprint FERMILAB-CONF-12-318-E, arXiv:1207.0449 [hep-ex] (2012).
 - [2] F. Englert and R. Brout, Phys. Rev. Lett. **13**, 321 (1964); P.W. Higgs, Phys. Rev. Lett. **13**, 508 (1964); G.S. Guralnik, C.R. Hagen, and T.W.B. Kibble, Phys. Rev. Lett. **13**, 585 (1964).
 - [3] S.L. Glashow, Nucl. Phys. **22**, 579 (1961); S. Weinberg, Phys. Rev. Lett. **19**, 1264 (1967); A. Salam (1968) in N. Svartholm. ed. *Eighth Nobel Symposium: Stockholm* [Almqvist and Wiksell, pp. 367].
 - [4] See, for example, S. P. Martin, “A Supersymmetry Primer,” (in Kane, G.L. (ed.): “Perspectives on supersymmetry II”, p.1), [hep-ph/9709356]; M. Drees, R. Godbole and P. Roy, “Theory and phenomenology of sparticles” (Hackensack, USA: World Scientific, 2004); H. Baer and X. Tata, “Weak scale supersymmetry,” (CUP, 2006).
 - [5] W. Beenakker, R. Hopker and M. Spira, hep-ph/9611232.
 - [6] R. Aaij *et al.* [LHCb Collaboration], Phys. Rev. Lett. **110**, 021801 (2013) [arXiv:1211.2674 [Unknown]].
 - [7] I. Adachi *et al.* [Belle Collaboration], arXiv:1208.4678 [hep-ex].
 - [8] J. Beringer *et al.* (Particle Data Group), Phys. Rev. D **86**, 010001 (2012).
 - [9] D. Ghosh, M. Guchait, S. Raychaudhuri and D. Sengupta, Phys. Rev. D **86**, 055007 (2012) [arXiv:1205.2283 [hep-ph]].
 - [10] A. Arbey, M. Battaglia, A. Djouadi, F. Mahmoudi and J. Quevillon, Phys. Lett. B **708**, 162 (2012) [arXiv:1112.3028 [hep-ph]]; A. Arbey, M. Battaglia, F. Mahmoudi and D. M. Santos, arXiv:1212.4887 [hep-ph]; W. Altmannshofer, M. Carena, N. R. Shah and F. Yu, arXiv:1211.1976 [hep-ph];
 - [11] J. R. Ellis, T. Falk, K. A. Olive and Y. Santoso, Nucl. Phys. B **652**, 259 (2003) [hep-ph/0210205].
 - [12] J. Ellis and K. A. Olive, Eur. Phys. J. C **72**, 2005 (2012) [arXiv:1202.3262 [hep-ph]]; P. Bechtle, T. Bringmann, K. Desch, H. Dreiner, M. Hamer, C. Hensel, M. Kramer and N. Nguyen *et al.*, JHEP **1206**, 098 (2012) [arXiv:1204.4199 [hep-ph]]; A. Fowlie, M. Kazana, K. Kowalska, S. Munir, L. Roszkowski, E. M. Sessolo, S. Trojanowski and Y. -L. S. Tsai, Phys. Rev. D **86**, 075010 (2012) [arXiv:1206.0264 [hep-ph]]; H. Baer, V. Barger, P. Huang, D. Mickelson, A. Mustafayev and X. Tata, arXiv:1210.3019 [hep-ph]; K. Kowalska, L. Roszkowski and E. M. Sessolo, arXiv:1302.5956 [hep-ph]; M. Carena, S. Gori, N. R. Shah, C. E. M. Wagner and L. -T. Wang, arXiv:1303.4414 [hep-ph]; A. Arbey, M. Battaglia and F. Mahmoudi, arXiv:1303.7450 [hep-ph].
 - [13] O. Buchmueller, R. Cavanaugh, M. Citron, A. De Roeck, M. J. Dolan, J. R. Ellis, H. Flacher and S. Heinemeyer *et al.*, Eur. Phys. J. C **72**, 2243 (2012) [arXiv:1207.7315 [hep-ph]]; S. Antusch, L. Calibbi, V. Maurer, M. Monaco and M. Spinrath, JHEP **01**, 187 (2013) [arXiv:1207.7236 [hep-ph]]; C. Strege, G. Bertone, F. Feroz, M. Fornasa, R. R. de Austri and R. Trotta, arXiv:1212.2636 [hep-ph]. J. Ellis, F. Luo, K. A. Olive and P. Sandick, arXiv:1212.4476 [hep-ph].
 - [14] U. Chattopadhyay and P. Nath, Phys. Atom. Nucl. **65**,

- 2101 (2002) [Yad. Fiz. **65**, 2165 (2002)] [hep-ph/0108250]; J. P. Miller, E. de Rafael and B. L. Roberts, Rept. Prog. Phys. **70**, 795 (2007) [hep-ph/0703049].
- [15] A. Djouadi, M. M. Muhlleitner and M. Spira, Acta Phys. Polon. B **38**, 635 (2007) [hep-ph/0609292].
- [16] F. Mahmoudi, Comput. Phys. Commun. **180**, 1579 (2009) [arXiv:0808.3144 [hep-ph]].
- [17] M. Frank, T. Hahn, S. Heinemeyer, W. Hollik, H. Rzehak and G. Weiglein, JHEP **0702**, 047 (2007) [hep-ph/0611326]; G. Degrandi, S. Heinemeyer, W. Hollik, P. Slavich and G. Weiglein, Eur. Phys. J. C **28**, 133 (2003) [hep-ph/0212020]; S. Heinemeyer, W. Hollik and G. Weiglein, Eur. Phys. J. C **9**, 343 (1999) [hep-ph/9812472]; S. Heinemeyer, W. Hollik and G. Weiglein, Comput. Phys. Commun. **124**, 76 (2000) [hep-ph/9812320].
- [18] C. Cheung, L. J. Hall, D. Pinner and J. T. Ruderman, arXiv:1211.4873 [hep-ph].
- [19] A. Arbey, M. Battaglia, A. Djouadi and F. Mahmoudi, arXiv:1211.4004 [hep-ph].
- [20] D. Asner *et al.* [Heavy Flavor Averaging Group Collaboration], arXiv:1010.1589 [hep-ex].
- [21] Y. Yook [BELLE Collaboration], talk given at ICHEP 2012.
- [22] B. Bhattacharjee, A. Dighe, D. Ghosh and S. Raychaudhuri, Phys. Rev. D **83**, 094026 (2011) [arXiv:1012.1052 [hep-ph]].
- [23] F. Ambrosino *et al.* [KLOE Collaboration], Phys. Lett. B **632**, 76 (2006) [hep-ex/0509045].
- [24] E. Lunghi, W. Porod and O. Vives, Phys. Rev. D **74**, 075003 (2006) [hep-ph/0605177].
- [25] [ATLAS Collaboration], ATLAS-CONF-2013-001 (2013).
- [26] [ATLAS Collaboration], ATLAS-CONF-2013-034 (2013).
- [27] [CMS Collaboration], CMS-PAS-HIG-13-003 (2013).
- [28] [CMS Collaboration], CMS-PAS-HIG-13-002 (2013).
- [29] [CMS Collaboration], CMS-PAS-HIG-13-053 (2013).
- [30] [CMS Collaboration], CMS-PAS-HIG-13-001 (2013).